HHS Public Access

Author manuscript

Chem Phys Lipids. Author manuscript; available in PMC 2020 May 11.

Published in final edited form as:

Chem Phys Lipids. 2019 May ; 220: 6–13. doi:10.1016/j.chemphyslip.2019.02.003.

Structural characterization of styrene-maleic acid copolymer-lipid nanoparticles (SMALPs) using EPR spectroscopy

Avnika P. Bali, **Indra D. Sahu**, **Andrew F. Craig**, **Emily E. Clark**, **Kevin M. Burridge**, **Madison T. Dolan**, **Carole Dabney-Smith**, **Dominik Konkolewicz***, **Gary A. Lorigan***

Department of Chemistry and Biochemistry, Miami University, Oxford, OH, 45056, USA

Abstract

Spectroscopic studies of membrane proteins (MPs) are challenging due to difficulties in preparing homogenous and functional lipid membrane mimetic systems into which membrane proteins can properly fold and function. It has recently been shown that styrene-maleic acid (SMA) copolymers act as a macromolecular surfactant and therefore facilitate the formation of disk-shaped lipid bilayer nanoparticles (styrene-maleic acid copolymer-lipid nanoparticles (SMALPs)) that retain structural characteristics of native lipid membranes. We have previously reported controlled synthesis of SMA block copolymers using reversible addition-fragmentation chain transfer (RAFT) polymerization, and that alteration of the weight ratio of styrene to maleic acid affects nanoparticle size. RAFT-synthesis offers superior control over SMA polymer architecture compared to conventional radical polymerization techniques used for commercially available SMA. However, the interactions between the lipid bilayer and the solubilized RAFT-synthesized SMA polymer are currently not fully understood. In this study, EPR spectroscopy was used to detect the perturbation on the acyl chain upon introduction of the RAFT-synthesized SMA polymer by attaching PC-based nitroxide spin labels to the 5^{th}, 12^{th}, and 16^{th} positions along the acyl chain of the lipid bilayer. EPR spectra showed high rigidity at the 12^{th} position compared to the other two regions, displaying similar qualities to commercially available polymers synthesized via conventional methods. In addition, central EPR linewidths and correlation time data were obtained that are consistent with previous findings.

Keywords

Styrene-maleic acid copolymers; SMALPs; Lipid bilayer; Electron paramagnetic resonance; CW-EPR; POPC vesicles

*Corresponding authors. konkold@miamioh.edu (D. Konkolewicz), gary.lorigan@miamioh.edu (G.A. Lorigan).

Competing financial interest

The authors declare no competing financial interest.

Appendix A. Supplementary data

Supplementary data associated with this article can be found, in the online version, at https://doi.org/10.1016/j.chemphyslip.2019.02.003.

1. Introduction

Membrane proteins (MP's) account for approximately 30% of the entire human genome and over 50% of current drug targets (Overington et al., 2006; Zheng et al., 2006). Thus, a better understanding of the structure of these proteins is imperative in order to develop more selective drugs that better target specific binding sites. Major structural methods such as magnetic resonance spectroscopy when combined with SMALP would widen its application to MPs. The presence of a native-like lipid environment is essential to maintaining the structure and function of MPs *in vitro* (Sachs and Engelman, 2006).

Multiple lipid membrane mimetics currently exist for the purpose of studying MPs, each with its own significant drawbacks. The most common technique is to use detergents to form spherical micelles in aqueous solution. However, detergent micelles do not provide the lipid bilayer structure which is important for MP structure and function, and are therefore not ideal native-like membrane mimetics. (Garavito and Ferguson-Miller, 2001; Seddon et al., 2004)

Liposomes, bicelles, nanodiscs, and lipodisq nanoparticles (non-RAFT SMALPs) formed from styrene-maleic acid copolymers are examples of several membrane mimetics that mimic a lipid bilayer structure (Seddon et al., 2004; De Angelis and Opella, 2007; Bayburt and Sligar, 2010; Sahu et al., 2013a, b; Sahu et al., 2017b, 2014). Liposomes, however, are often inhomogeneous in size, have inaccessible interiors, and exhibit limited solubility in aqueous solutions (Raschle et al., 2010). The major disadvantage of liposomes is their large size. Bicelles also display size heterogeneity, and can be formed only with limited lipid-detergent combinations (Raschle et al., 2010). While nanodiscs can be formed with various types of lipids and have improved stability in comparison to other membrane mimetics, (Denisov et al., 2004) the presence of membrane scaffold proteins can interfere with the protein of interest, and detergent is still required to stabilize the protein prior to incorporation in the nanodisc (Bayburt and Sligar, 2010; Denisov et al., 2004; Bayburt and Sligar, 2003).

Recently, it has been shown that styrene-maleic acid (SMA) copolymers are able to facilitate the self-assembly of lipid discs that maintain the structural and dynamic properties of membrane proteins. The lipodisq™ nanoparticle (non-RAFT SMALPs) system serves as a common example of SMA polymers being used for structural analysis of membrane proteins (Sahu et al., 2013a; Orwick-Rydmark et al., 2012; Orwick et al., 2012). These styrene-maleic acid copolymer-lipid nanoparticles (SMALPs) exhibit a lipid bilayer structure, and can be formed homogenously in solution. In addition, SMALPs can be formed in a detergent-free environment, unlike nanodiscs, which require membrane scaffolding proteins. One highly advantageous aspect of the SMALP complex is its disk-like shape, which grants access to both intra- and extracellular domains of membrane protein. In addition, the SMA-stabilized lipid samples can exhibit higher homogeneity than other lipid mimetics, and the absence of large quantities of detergent make this model more preferable than micelles or bicelles.

The synthesis of SMA begins with the copolymerization of styrene and maleic anhydride in order to form styrene-maleic anhydride (SMAnh), which is then hydrolyzed, yielding SMA. However, commercially available samples of SMA/SMAnh copolymers consist of highly variable molecular weights, due to the use of conventional radical polymerization. When synthesized using conventional radical polymerization techniques, SMA typically has a dispersity in the range of 2.0–2.5 range, (Baruah and Laskar, 1996; Dorr et al., 2016) indicating a broad distribution of polymer chain size. In addition, conventional radical polymerization offers limited control over the architecture and composition of the polymer.

Previous studies have reported the controlled synthesis and initial characterization of styrene-maleic acid copolymer-lipid nanoparticles (SMALPs) (Craig et al., 2016; Smith et al., 2017; Hall et al., 2018; Pardo et al., 2018, 2017). However, further characterization of interaction between the lipid bilayer and the solubilized SMA polymer has not been conducted. Here, we examine the effect of the presence of SMA polymers on the lipid bilayers they stabilize using continuous-wave EPR spectroscopy. CW-EPR spectroscopy is a well-established method for probing the changes in the physical structure of the lipids resulting from the introduction of an external molecule (Sahu et al., 2013b; Sahu and Lorigan, 2015, 2018). The SMA polymer is known to bind to the hydrophobic core of the lipid bilayer (Sahu et al., 2017a; Orwick et al., 2012; Craig et al., 2016). EPR spectroscopy can detect the perturbation on the acyl chain upon the introduction of the SMA polymer using PC-based nitroxide spin labels attached to different carbons in the hydrocarbon chain. This approach was previously used to investigate many factors that modify fluidity of the membrane, such as cholesterol, carotenoids, peptides and membrane proteins. (Dorr et al., 2016; Craig et al., 2016) In this study, liposomes were used as a reference model and compared to SMALPs. The addition of spin labeled fatty acids to liposomes treated with the SMA polymer allows for a direct comparison of the mobility at different depths of the acyl chain between liposomes and SMALPs. Membrane fluidity increases at higher temperature causing more dynamic motion for the embedded membrane protein. In this study, we used two different temperatures (296 K (23 °C) and 318 K (45 °C)) to characterize the effect of the SMA on different motional membrane environments for EPR spectroscopic studies.

2. Experimental section

2.1. Materials

1-Palmitoyl-2-oleoyl-sn-glycero-3-phosphocholine (POPC) was purchased from Avanti Polar Lipids (Alabaster, Alabama, USA)). 5, 12 and 16 DOXYL stearic acid spin labels and N-[2- Hydroxyethyl]Piperazine-N′-2-ethanesulfonic acid (HEPES) were purchased from Sigma-Aldrich (St. Louis, MO, USA). Sodium chloride (NaCl) was purchased from Fisher Scientific (Pittsburgh, PA, USA).

2.2. Synthesis of styrene maleic anhydride copolymer

SMA synthesis was conducted as previously described by Craig et al. (Craig et al., 2016), beginning with the synthesis of 2-(((dodecylthio) carbonothioyl)thio)propanoic acid or (2-propionic acid)yl dodecyl trithiocarbonate (PADTC).

A solution of sodium hydroxide (7.50 g, 0.19 mol) was prepared in 75 mL of water and added dropwise to the solution of DDT (37.5 g, 0.19 mol) and TPAB (4.10 g, 0.018 mol) in acetone (600 mL). The reaction mixture was stirred and placed in an ice bath and treated with carbon disulfide (11.4 mL, 14.4 g, 0.19 mol) to give sodium dodecyl-trithiocarbonate. This solution was stirred and treated with BPA (17 mL, 28.7 g, 0.19 mol). The resulting solution was stirred overnight at room temperature and purified by precipitation with HC1 and vacuum filtration and recrystallization at −18 °C. The resulting yellow crystals were isolated by vacuum filtration to give PADTC.

One pot block copolymers of poly(styrene-*alt*-maleic anhydride-*b*-styrene) were then synthesized by mixing PADTC (70.2 mg, 0.200 mmol), AIBN (6.2 mg, 0.038 mmol), maleic anhydride (0.980 g, 10.0 mmol) and styrene (4.16 g, 40.0 mmol) in a glass vial, followed by dioxane (5.62 mL). The solution was placed in an ice bath and deoxygenated by bubbling with nitrogen for 10 min, and was then placed in an oil bath and allowed to polymerize at 65 °C for 16 h. The polymer was purified by precipitation two times into hexane at 0 °C.

Next, RAFT End-group removal was conducted with a short styrene block to the poly(styrene-*alt*-maleic anhydride-*b*-styrene). 3.6 g of polymer, 0.26 mmol trithiocarbonate) was dissolved in dioxane. BPO (2.4 g, 9.9 mmol) was mixed to the solution, which was then placed in an ice bath, deoxygenated by bubbling with nitrogen for 10 min, then placed in an oil bath at 80 °C for 4 h, 20 min. The polymer was purified by 3 times precipitation into hexanes at 0 °C.

2.3. Size exclusion chromatography (SEC) procedure

Approximately 5 mg of polymer was weighed out and dissolved in 1.5 mL THF with 0.025% butylated hydroxy toluene (BHT), to this mixture was added two drops of toluene as a flow rate marker. The solution was filtered through a 0.22 μm filter. Size exclusion chromatography was performed using an Agilent 1260 gel permeation chromatography system equipped with an autosampler, a guard and 2 × PL Gel Mixed B columns, and a refractive index detector. The eluent was tetrahydrofuran running at 1 mL/min at 25 °C. The system was calibrated with poly(methyl methacrylate) standards in the range of 617,000–1010 and corrected to polystyrene using the standard Mark-Houwink parameters K_{MMA} = 12.8, α_{MMA} = 0.69, K_{Sty} = 11.4, α_{Sty} = 0.716. The M_n by GPC, after applying the Mark-Houwink correction for polystyrene was 7.0 kDa, M_w of 9.8 kDa, with a polydispersity of 1.40. The probability distribution of molecular weight of styrene-maleic acid (SMA) copolymer is given in the supporting information in Figure S1. The polymer structure is a very close approximation to what is drawn due to the very high cross-reactivity ratios between styrene and maleic anhydride. Styrene reacts with itself much slower than with maleic anhydride, so it is assumed that an excess of styrene leads to an alternating segment followed by a hydrophobic tail composed of the remaining styrene. This is, however, an approximation; detailed Monte Carlo analysis done by Ting Xu's group shows that the degree of alternation decreases as anhydride is consumed (see Ref. (Smith et al., 2017). A more precise description of these RAFT-synthesized copolymers is that they are gradient copolymers with a very steep gradient, as opposed to block copolymers. However due to the steep gradient, the "block" description has been a satisfactory one thus far. Precise NMR

characterization of these copolymers, to our knowledge, has not been done. This is mainly due to the significant broadening observed when the maleic anhydride protons are incorporated into the polymer backbone; meaningful resolution of these protons cannot be obtained. The NMR data on polymer structure are shown in the supporting information in Figure S2. The two carboxyl groups in a maleic acid unit have different pKa values: the first pKa is close to 4.7, whereas the second is close to 9.2 (see the titration curve Figure S3).This is consistent with previously published pKa values of SMA (Dorr et al., 2016).

2.4. Styrene-Maleic anhydride copolymer hydrolysis

Organic soluble styrene-maleic anhydride copolymers were solubilized in a small amount of tetrahydropfuran (THF). Hydrolysis of maleic anhydride to maleic acid was performed by adding 4X molar excess of NaOH (Fisher Bioreagents) drop wise to the THF solution at room temperature. Hydrolysis was allowed to proceed overnight at room temperature and added to 3.5 kDa dialysis tubing (Spectrum Labs Rancho Dominguez, CA, USA) in 1 L of ddH_2O to remove unreacted base. The resulting SMA copolymer solution was then removed from dialysis tubing, flash-frozen in liquid nitrogen, and lyophilized. Resulting powders were stored at room temperature for future use.

2.5. Preparation of POPC vesicles and SMALPs

POPC was purchased from Avanti Polar Lipids, and 5, 12, and 16-doxyl stearic acid spin labels were purchased from Sigma Aldrich. Lipodisq nanoparticles (pre-hydrolyzed styrene-maleic anhydride copolymer 3:1 ratio) (non-RAFT commercial polymer) were obtained from Sigma-Aldrich. Powdered POPC was mixed with 1 mol% of lipid spin label in chloroform and then dried under a stream of nitrogen gas. The resulting lipid film was put under vacuum for 24 h. The dried lipids were suspended in 100 mM NaCl, 20 mM HEPES (pH 7.0), vortexed, and subjected to ten freeze–thaw cycles, after which it was centrifuged at 13 000 *g*, for 30 min at 4 °C.

SMA polymers were dissolved in 100 mM NaCl, 20 mM HEPES (pH 7.0) to a final concentration of 5% (m/v), and sonicated for 1 min, allowing for complete dissolution. SMALPs were formed by adding the SMA polymer solution drop-wise into the POPC vesicle solution at a 1/1 wt ratio. Samples were then equilibrated via two freeze/thaw cycles and were mixed overnight at room temperature. Samples were then centrifuged at 20,000 g for 30 min to remove aggregates prior to taking EPR measurements. The presence of the minor amount of free SMA may increase the viscosity of the sample solution that may not significantly influence the relative motion of spin labels in CW-EPR measurements. (Sahu et al., 2013a, b; Sahu et al., 2017b, 2014; Orwick et al., 2012).

2.6. Nuclear magnetic resonance (NMR) spectroscopic measurements

Monomer conversion during polymer synthesis was determined by Nuclear Magnetic Resonance (NMR) on a Bruker 300 MHz or 500 MHz NMR spectrometer. Pre-hydrolysis polymer was dissolved in DMSO-d_6 and the spectrum was collected on a Bruker 500 MHz spectrometer. Hydrolyzed polymer was insoluble in DMSO-d_6 alone, but easily dissolved after addition of a single drop of 6 M HCl.

2.7. EPR measurements

CW-EPR spectra were collected at X-band on a Bruker EMX CW-EPR spectrometer using an ER041xG microwave bridge and ER4119-HS cavity coupled with a BVT 3000 nitrogen gas temperature controller. Each spin-labeled CW-EPR spectrum was acquired by signal averaging 20 42-s field scans with a central field of 3315 G and sweep width of 100 G, modulation frequency of 100 kHz, modulation amplitude of 1 G, and microwave power of 10 mW at temperatures 296 K and 318 K. Data were analyzed using the methods outlined in the literature. (Stepien et al., 2015; Camargos and Alonso, 2013; Tan et al., 2015) The order parameters were calculated using $S = 0.5407 \times (A_{max} - A_{min})/a_0$, $a_0 = (A_{max} + 2A_{min})/3$, where A_{max} and A_{min} are maximum and minimum hyperfine interaction parameters (Tan et al., 2015). Figure S4 shows the measurement of A_{max} and A_{min} from an EPR spectrum. The membrane has a crystal structure when the order parameter (S) is equal to 1. If the order parameter is equal to zero, the membrane is in total disorder.

2.8. EPR spectral simulations

EPR spectra were simulated using the non-linear least squares (NLSL) program including the macroscopic order, microscopic disorder (MOMD) model developed by the Freed group (Schneider and Freed, 1989; Budil et al., 1996) following similar method suggested in the literature (Camargos and Alonso, 2013). The principle components of the hyperfine interaction tensor A = [6.6 ± 0.5, 5.5 ± 0.5, 33.7 ± 0.8] G and g-tensors g = [2.0078 ± 0.0002, 2.0058 ± 0.0004, 2.0025 ± 0.0001] for sitel and A = [5.3 ± 0.5, 6.4 ± 0.5, 34.9 ± 0.8] G and g-tensors g = [2.0084 ± 0.0002, 2.0063 ± 0.0004,2.0023 ± 0.0001] for site 2 were obtained from the literature and tightly refined to fit the EPR spectra (Camargos and Alonso, 2013). During the simulation process, the rotational diffusion tensors were varied. A two-site fit was used to account for both rigid/slower and higher/faster motional components of the EPR spectrum. The best fit rotational correlation times and the relative population of both components were determined using the Brownian diffusion model.

3. Results and discussion

Recently, we characterized the structure and size of RAFT-synthesized SMALPs via dynamic light scattering (DLS), transmission electron microscopy (TEM), and nuclear overhouser effect spectroscopy (NOESY) nuclear magnetic resonance (NMR) spectroscopy (Craig et al., 2016; Zhang et al., 2015, 2017). Such characterization studies found that altering the SMA/lipid weight ratio effectively tunes the size of the lipid disk (Craig et al., 2016), showing the potential utility of RAFT SMALPs for biophysical studies of membrane proteins at different nanoscale sizes. This study further characterizes the polymer-lipid interaction in RAFT-synthesized SMALPs using CW-EPR line shape analysis. RAFT SMALPs were formed from POPC liposomes, since POPC has been shown to mimic the phospholipids in mammalian membranes (Craig et al., 2016; Zhang et al., 2015; Sahu et al., 2015; Barrett et al., 2012). Fig. 1 shows a chemical structure of the DOXYL spin label as well as the cartoon representation of the addition of a SMA polymer to an intact vesicle to form the membrane RAFT SMALP.

3.1. Effect of RAFT-synthesized SMALPs on lipid chain mobility

CW-EPR spectra of spin-labeled molecules is highly responsive to changes in the motion of spin label side chains. (Sahu et al., 2013b; Sahu and Lorigan, 2015, 2018; Klug and Feix, 2008) The degree of mobility of the DOXYL spin label group can be obtained by line-shape analysis of CW-EPR spectra. Fig. 2 shows CW-EPR spectra collected for the spin label attached at the 5^{th}, 12^{th}, and 16^{th} carbon of the lipid chain at temperatures 296 K (middle panel) and 318 K (right panel). Fig. 2 indicates that some of the CW-EPR spectra contain two motional components, indicated by downward arrows. The left arrow indicates a slower/ rigid component and the right arrow indicates a faster motional component. Inspection of the EPR spectra indicates a broader lineshape for the spin label at the 5^{th} acyl chain when compared to the 12^{th} and 16^{th} acyl chain positions at 296 K. Upon addition of the SMA polymer to lipid vesicles, EPR spectra taken at the 5^{th} and 12^{th} carbon of the acyl chain undergo increase in line broadening with an increase in the slow/ rigid component at 296 K (Figs. 3 A and B middle panel). At 318 K, CW EPR lineshape broadening decreases for the 5^{th} and 12^{th} spin label positions for both vesicle and SMALP samples. The slow/rigid component is significantly reduced which is perhaps due to the signal averaging of the two motional components at the higher temperature. (Sahu et al., 2017a; Ghimire et al., 2012) The CW-EPR spectra for the spin label at the 16^{th} carbon of the acyl chain does not have two motional components for vesicles as well as SMALP samples at both temperatures, which may be due to the decrease in the restriction provided by the acyl chain on the spin label at the center of lipid bilayers.

The mobility of the 5^{th}, 12^{th}, and 16^{th} carbon of the lipid chain was probed further using well established spectral parameters; the central linewidth (H_0), and spectral width ($2A_{zz}$). An increase in these parameters is generally associated with decreased motional freedom of the spin label.

Fig. 3 represents a plot of the central linewidth of EPR spectra as a function of spin label position at temperatures 296 K and 318 K. The central linewidth varies between 2.02 G to 2.83 G for all the samples without the addition of SMA and 2.12 G to 3.96 G with the addition of SMA at 296 K. Similarly, the central linewidth varies between 1.56 G to 2.36 G for all the samples without the addition of SMA and 1.67 G to 2.62 G with the addition of SMA at 318 K. Fig. 4 shows the plot of the spectral width ($2A_{zz}$) of the EPR spectra as a function of spin label position at temperatures 296 K and 318 K. The spectral width ($2\ A_{zz}$) varies between 31.9 G to 52.9 G for all the samples without the addition of SMA and 32.6 G to 58.9 G with the addition of SMA at 296 K. Similarly, the spectral width ($2\ A_{zz}$) varies between 30.8 G to 45.5 G for all the samples without the addition of SMA and 30.8 G to 49.2 G with the addition of SMA at 318 K.

Fig. 5 shows the plot of order parameter (S) of the EPR spectra as a function of spin label position at temperatures 296 K and 318 K. The highest value of S (equal to 1) represents the crystal structure of the membrane, while the lowest value of S (equal to 0) represents that the membrane is in total dynamic disorder. The order parameter (S) varies between 0.13 to 0.60 for all the samples without the addition of SMA and 0.17 to 0.62 with the addition of SMA at 296 K. Similarly, the order parameter (S) varies between 0.08 to 0.48 for all the samples without the addition of SMA and 0.09 to 0.54 with the addition of SMA at 318 K. As

indicated by the comparison of parameters at each position (Fig. 3 and 4), the 12th carbon seems to exhibit the highest degree of immobility upon introduction of the SMA polymer when compared to positions 5 and 16. This indicates that the fatty acid chain mobility near the polar headgroups of the SMALPs remain fairly unchanged upon addition of SMA. However, carbons in the middle of the fatty acid chain (near the 12th carbon), are much more immobile when interacting with the SMA. No significant changes were observed in the dynamics of the DOXYL spin label at the 16th carbon position, indicating absence of polymer dynamic interaction at this site. As indicated in Fig. 5, the value of the order parameters (S) increased for all the acyl chain sites with the addition of SMA indicating an increase in membrane ordering with the formation of SMALPS. The higher increase in the order parameters of the 12 position in SMALPs than in liposomes (Fig. 5) suggest that the SMALPs exert pressure on the lipid bilayer during stabilization, causing them to pack in more order.

In order to further characterize the two motional components observed in the CW EPR spectra, we performed non-linear least squares (NLSL) simulations on representative CW-EPR spectra at 12 acyl chain position in the absence of SMA and in the presence of SMA as shown in Fig. 6. The simulation result indicated that the motion of the acyl chain at 12 position is slower with a rotational correlation time of 22 ns and a relative population of 74% (rigid component) and 13 ns of 26% (motional component) with the addition of SMA when compared to the rotational correlation time of 18 ns with a relative population of 76% (rigid component) and 7 ns of 24% (motional component) without the addition of SMA at 296 K. Similarly, the motion of the spin label at position 12 is slower with a rotational correlation time of 11 ns and a relative population of 73% (rigid component) and 4 ns of 27% (motional component) with the addition of SMA when compared to the rotational correlation time of 7 ns with relative population of 79% (rigid component) and 3 ns of 21% (motional component) without the addition of SMA at 318 K. The slower motion of the spin labels in the presence of SMA are consistent with the previously reported data on lipid-SMA systems. (Sahu et al., 2013a, b; Sahu et al., 2017b; Orwick-Rydmark et al., 2012; Orwick et al., 2012), The decrease in motion of the spin labeled acyl chain at position 12 in the presence of SMA is also consistent with our spin label mobility data, spectral width data and order parameters reported in this study. The phase transition temperature of POPC lipid is −2 °C. This suggests that the lipid acyl chains are in the fluid state at 296 K, but are more mobile at 318 K. The decrease in order parameters for the samples at 318 K indicates that the lipid acyl chains are loosely packed due to increase in membrane fluidity at higher temperature leading to a lower ordering of lipid molecules when compared at 296 K.

CW-EPR spectra obtained for the spin labeled carbon position 5-DOXYL stearic acid of SMALPs samples prepared from the commercial SMA polymer were compared to the CW-EPR spectra obtained from RAFT-SMA at 296 K (23 °C) and 318 K (45 °C) (see Figure S5). The comparison of the data indicated comparable EPR spectral lineshape broadenings from vesicles to SMALP samples at both temperatures. Commercial polymer using spin labeled PC in DMPC vesicles has been already characterized using EPR spectroscopy by the Watts group. [16] EPR studies published by the Watts group showed the CW-EPR spectral line broadening increases on the spin labeled PC in DMPC in the presence of SMA polymer when compared to that in vesicles. Our EPR data on SAMLPs are consistent with the EPR

data reported on the commercial polymer. [16] The additional EPR spectral line broadenings for the samples might be due to a decrease in the motion of lipid acyl chain in the presence of the SMA polymer while forming the SMALPs resulting in a decrease in the motion of the spin-labels. The SMALPs system is formed due to the lateral pressure generated due to the polymer and lipid chain interaction isolating the individual complex with specific smaller size (Orwick et al., 2012). Recent studies have indicated that the SMA polymer forms like a bracelet around the lipid membrane with the styrene moieties oriented parallel to the membrane normal and interacting directly with the lipid acyl chain while maleic acid groups are oriented in the same direction of styrene moieties and interacting with the lipid head groups (Jamshad et al., 2015). The driving force for the spontaneous formation of the SMALPs towards the burial of the styrene groups into the hydrophobic core of the membrane might be contributing towards the decrease of lipid acyl chain motion.

The location of SMA polymer interaction with the hydrophobic region is consistent with conventional membrane scaffolding proteins used in the formation of nanodiscs (Stepien et al., 2015). In addition, this is consistent with the binding region of commercially available SMA polymers used for the lipodisq™ system (non-RAFT SMALPs) (Orwick et al., 2012).

These structural studies show insight into how RAFT-synthesized SMA alters the physical structure of the liposomal lipid bilayer. SMALPs offer enhanced control over lipid disk size by controlling composition of the SMA polymer, making this system ideal for structural NMR studies. Our previous study suggested that the particle size changes depending on the styrene:anhydride ratios (Craig et al., 2016; Hall et al., 2018). Our previous DLS and TEM data also suggested the average sizes of the SMALPs formed by copolymer (styrene:maleic acid = 3:1) are 10–12 ns (Craig et al., 2016; Harding et al., 2019). There is no significant difference in the particle size with the spin labeled SMALPs and without the spin labeled SMALPs as well as before and after EPR measurements (Sahu et al., 2017a, b; Orwick-Rydmark et al., 2012; Orwick et al., 2012). Recently, characterization of the integral membrane protein KCNE1 inserted into lipid disks stabilized by the lipodisq™ copolymer type (non-RAFT SMALPs) was conducted in the transmembrane and extra-membrane domains, with structural results that were consistent with the solution NMR structure (Sahu et al., 2017a). Membrane protein characterization studies have yet to be conducted in SMALPs stabilized by RAFT-synthesized SMA copolymers. Recently, Xue et al. investigated the molecular mechanism of the formation of SMALPs using coarse-grained molecular dynamics simulations and suggested that the SMALP nanodisks are the thermodynamically favorable state of the system (Xue et al., 2018). The decrease in the motion of the spin labeled PC in the presence of the SMA copolymer observed in this study is consistent with our previous EPR spectroscopic studies on the KCNE1 membrane protein incorporated into lipodisq nanoparticles (non-RAFT SMALPs). (Sahu et al., 2017a; Sahu et al., 2017b) This study and our previous studies suggest that the overall reduction in the global motion of the SMALPs complex may help to determine the local dynamics of spin probes. The reduction in the global motion of the complex may also help to understand the backbone motion of the protein incorporated into SMALPs. (Sahu et al., 2017a; Sahu et al., 2017b) A future study is required to further characterize the SMALPs in the presence of integral membrane proteins and formation of SMALPs using different lipid types. Isothermal titration calorimetry (ITC) and differential scanning calorimetry (DSC) may

further answer the question of whether the spin-label itself has perturbed the thermal behavior of the lipids during the formation of SMALPs and complement this study.

4. Conclusion

In this study, we showed that changes introduced into lipid bilayer upon the addition of SMA are indeed not negligible, and should be considered before using this membrane model for membrane protein studies. Characterization of the RAFT-synthesized copolymer type will be useful as a comparison to existing copolymer systems, in order to assist in choosing the optimal membrane mimetic environment for a given membrane protein.

Supplementary Material

Refer to Web version on PubMed Central for supplementary material.

Acknowledgements

This work was generously supported by the NIGMS/NIH Maximizing Investigator's Research Award (MIRA)R35GM126935 Award and a NSF CHE-1807131 grant. The pulsed EPR spectrometer was purchased through funding provided by the NSF (MRI-1725502), the Ohio Board of Reagents, and Miami University. Gary A. Lorigan would also like to acknowledge support from the John W. Steube Professorship.

Funding sources

National Institutes of Health GrantR01GM108026.

National Science Foundation GrantCHE-1807131.

References

Barrett PJ, Song Y, Van Horn WD, Hustedt EJ, Schafer JM, Hadziselimovic A, Reel AJ, Sanders CR, 2012 The amyloid precursor protein has a flexible transmembrane domain and binds cholesterol. Science 336 (6085).

Baruah SD, Laskar NC, 1996 Styrene-maleic anhydride copolymers: synthesis, characterization, and thermal properties. J. Appl. Polym. Sci 60 (5), 649–656.

Bayburt TH, Sligar SG, 2003 Self-assembly of single integral membrane proteins into soluble nanoscale phospholipid bilayers. Protein Sci. 12 (11), 2476–2481. [PubMed: 14573860]

Bayburt TH, Sligar SG, 2010 Membrane protein assembly into Nanodiscs. FEBS Lett. 584 (9), 1721–1727. [PubMed: 19836392]

Budil DE, Lee S, Saxena S, Freed JH, 1996 Nonlinear-Least-Squares Analysis of Slow-Motion EPR Spectra in One and Two Dimensions Using a Modified Levenberg-Marquardt Algorithm. J. Magn. Reson. A 120, 155–189.

Camargos HS, Alonso A, 2013 Electron paramagnetic resonance (epr) spectral components of spin-labeled lipids in saturated phospholipid bilayers. Effect of cholesterol. Quimica Nova 36 (6), 815–U152.

Craig AF, Clark EE, Sahu ID, Zhang R, Frantz ND, Al-Abdul-Wahid S, Dabney-Smith C, Konkolewicz D, Lorigan GA, 2016 Tuning the size of styrene-maleic acid copolymer-lipid nanoparticles (SMALPs) using RAFT polymerization for biophysical studies. Biochim. Biophys. Acta 1858, 2931–2939. [PubMed: 27539205]

De Angelis AA, Opella SJ, 2007 Bicelle samples for solid-state NMR of membrane proteins. Nat. Protoc 2 (10), 2332–2338. [PubMed: 17947974]

Denisov IG, Grinkova YV, Lazarides AA, Sligar SG, 2004 Directed self-assembly of monodisperse phospholipid bilayer nanodiscs with controlled size. J. Am. Chem. Soc 126 (11), 3477–3487. [PubMed: 15025475]

Dorr JM, Scheidelaar S, Koorengevel MC, Dominguez JJ, Schafer M, van Walree CA, Killian JA, 2016 The styrene-maleic acid copolymer: a versatile tool in membrane research. Eur. Biophys. J 45 (1), 3–21. [PubMed: 26639665]

Garavito RM, Ferguson-Miller S, 2001 Detergents as tools in membrane biochemistry. J. Biol. Chem 276 (35), 32403–32406. [PubMed: 11432878]

Ghimire H, Hustedt EJ, Sahu ID, Inbaraj JJ, McCarrick R, Mayo DJ, Benedikt MR, Lee RT, Grosser SM, Lorigan GA, 2012 Distance Measurements on a Dual-Labeled TOAC AChR M2S Peptide in Mechanically Aligned DMPC Bilayers via Dipolar Broadening CW-EPR Spectroscopy. J. Phys. Chem. B 116 (12), 3866–3873. [PubMed: 22379959]

Hall SCL, Tognoloni C, Price GJ, Klumperman B, Edler KJ, Dafforn TR, Arnold T, 2018 Influence of Poly(styrene-co-maleic acid) copolymer structure on the properties and self-assembly of SMALP nanodiscs. Biomacromolecules 19 (3), 761–772. [PubMed: 29272585]

Harding BD, Dixit G, Burridge KM, Sahu ID, Dabney-Smith C, Edelmann RE, Konkolewicz D, Lorigan GA, 2019 Characterizing the structure of styrene-maleic acid copolymer-lipid nanoparticles (SMALPs) using RAFT polymerization for membrane protein spectroscopic studies. Chem. Phys. Lipids 218, 65–72. [PubMed: 30528635]

Jamshad M, Grimard V, Idini I, Knowles TJ, Dowle MR, Schofield N, Sridhar P, Lin Y, Finka R, Wheatley M, Thomas ORT, Palmer RE, Overduin M, Govaerts C, Ruysschaert J-M, Edler KJ, Dafforn TR, 2015 Structural analysis of a nanoparticle containing a lipid bilayer used for detergent-free extraction of membrane proteins. Nano Res. 8 (3), 774–789. [PubMed: 31031888]

Klug CS, Feix JB, 2008 Methods and applications of site-directed spin labeling EPR spectroscopy. Methods Cell Biol. 84, 617–658. [PubMed: 17964945]

Orwick MC, Judge PJ, Procek J, Lindholm L, Graziadei A, Engel A, Grobner G, Watts A, 2012 Detergent-free formation and physicochemical characterization of nanosized lipid-polymer complexes: lipodisq. Angewandte Chemie-International Edition 51 (19), 4653–4657. [PubMed: 22473824]

Orwick-Rydmark M, Lovett JE, Graziadei A, Lindholm L, Hicks MR, Watts A, 2012 Detergent-free incorporation of a seven-transmembrane receptor protein into nanosized bilayer lipodisq particles for functional and biophysical studies. Nano Lett. 12 (9), 4687–4692. [PubMed: 22827450]

Overington JP, Al-Lazikani B, Hopkins AL, 2006 How many drug targets are there? Nat. Rev. Drug Discov 5 (12), 993–996. [PubMed: 17139284]

Pardo JJD, Dorr JM, Iyer A, Cox RC, Scheidelaar S, Koorengevel MC,Subramaniam V, Killian JA, 2017 Solubilization of lipids and lipid phases by the styrene-maleic acid copolymer. Eur. Biophys. J. Biophys. Lett 46 (1), 91–101.

Pardo JJD, Koorengevel MC, Uwugiaren N, Weijers J, Kopf AH, Jahn H, van Walree CA, van Steenbergen MJ, Killian JA, 2018 Membrane solubilization by styrene-maleic acid copolymers: delineating the role of polymer length. Biophys. J 115 (1), 129–138. [PubMed: 29972804]

Raschle T, Hiller S, Etzkorn M, Wagner G, 2010 Nonmicellar systems for solution NMR spectroscopy of membrane proteins. Curr. Opin. Struct. Biol 20 (4), 471–479. [PubMed: 20570504]

Sachs JN, Engelman DM, 2006 Introduction to the Membrane Protein Reviews: The Interplay of Structure, Dynamics, and Environment in Membrane Protein Function.

Sahu ID, Lorigan GA, 2015 Biophysical EPR studies applied to membrane proteins. J. Phys. Chem. Biophys 5 (6), 188. [PubMed: 26855825]

Sahu ID, Lorigan GA, 2018 Site-directed spin labeling EPR for studying membrane proteins. Biomed Res. Int

Sahu ID, MaCarrick RM, Troxel KR, Zhang R, Smith JH, Dunagan MM, Swartz MS, Rajan PV, Kroncke BM, Sanders CR, Lorigan GA, 2013a DEER EPR measurement for membrane protein structures via bifunctional spin labels and lipodisq nanoparticles. Biochemistry 52 (38), 6627–6632. [PubMed: 23984855]

Sahu ID, McCarrick RM, Lorigan GA, 2013b Use of electron paramagnetic resonance to solve biochemical problems. Biochemistry 52, 5967–5984. [PubMed: 23961941]

Sahu ID, Kroncke BM, Zhang R, Dunagan MM, Smith HJ, Craig A, McCarrick RM, Sanders CR, Lorigan GA, 2014 Structural Investigation of the transmembrane domain of KCNE1 in proteoliposomes. Biochemistry 53, 6392–6401. [PubMed: 25234231]

Sahu ID, Craig AF, Dunagan MM, Troxel KR, Zhang R, Meiberg AG, Harmon CN, MaCarrick RM, Kroncke BM, Sanders CR, Lorigan GA, 2015 Probing structural dynamics and topology of the KCNE1 membrane protein in lipid bilayers via Site-Directed Spin Labeling and Electron Paramagnetic resonance spectroscopy. Biochemistry 54, 6402–6412. [PubMed: 26418890]

Sahu ID, Zhang R, Dunagan MM, Craig A, Gary AL, 2017a Characterization of KCNE1 inside lipodisq nanoparticles for EPR spectroscopic studies of membrane proteins. J. Phys. Chem. B 121, 5312–5321. [PubMed: 28485937]

Sahu ID, Craig AF, Dunagum MM, McCarrick RM, Lorigan GA, 2017bCharacterization of bifunctional spin labels for investigating the structural and dynamic properties of membrane proteins using EPR spectroscopy. J. Phys. Chem. B 121 (39), 9185–9195. [PubMed: 28877443]

Schneider DJ, Freed JH, 1989 Calculating slow motional magnetic resonance spectra: a user's guide In: Berlinger LJ (Ed.), Biological Magnetic Resonance. Plenum Publishing, New York.

Seddon AM, Curnow P, Booth PJ, 2004 Membrane proteins, lipids and detergents: not just a soap opera. Biochim. Biophys. Acta 1666 (1-2), 105–117. [PubMed: 15519311]

Smith AAA, Autzen HE, Laursen T, Wu V, Yen M, Hall A, Hansen SD, Cheng YF, Xu T, 2017 Controlling styrene maleic acid lipid particles through RAFT. Biomacromolecules 18 (11), 3706–3713. [PubMed: 28934548]

Stepien P, Polit A, Wisniewska-Becker A, 2015 Comparative EPR studies on lipid bilayer properties in nanodiscs and liposomes. Biochimica Et Biophysica Acta- Biomembranes 1848 (1), 60–66.

Tan C, Zhang YT, Abbas S, Feng B, Zhang XM, Xia WS, Xia SQ, 2015Biopolymer-lipid bilayer interaction modulates the physical properties of liposomes: mechanism and structure. J. Agric. Food Chem 63 (32), 7277–7285. [PubMed: 26173584]

Xue MM, Cheng LS, Faustino I, Guo WL, Marrink SJ, 2018 Molecular mechanism of lipid nanodisk formation by styrene-maleic acid copolymers. Biophys. J 115 (3), 494–502. [PubMed: 29980293]

Zhang R, Sahu ID, Liu L, Osatuke A, Corner RG, Dabney-Smith C, Lorigan GA, 2015 Characterizing the structure of lipodisq nanoparticles for membrane protein spectroscopic studies. Biochimica Et Biophysica Acta-Biomembranes 1848 (1), 329–333.

Zhang RF, Sahu ID, Bali AP, Dabney-Smith C, Lorigan GA, 2017Characterization of the structure of lipodisq nanoparticles in the presence of KCNE1 by dynamic light scattering and transmission electron microscopy. Chem. Phys. Lipids 203, 19–23. [PubMed: 27956132]

Zheng C, Han L, Yap CW, Xie B, Chen Y, 2006 Progress and problems in the exploration of therapeutic targets. Drug Discov. Today 11 (9–10), 412–420. [PubMed: 16635803]

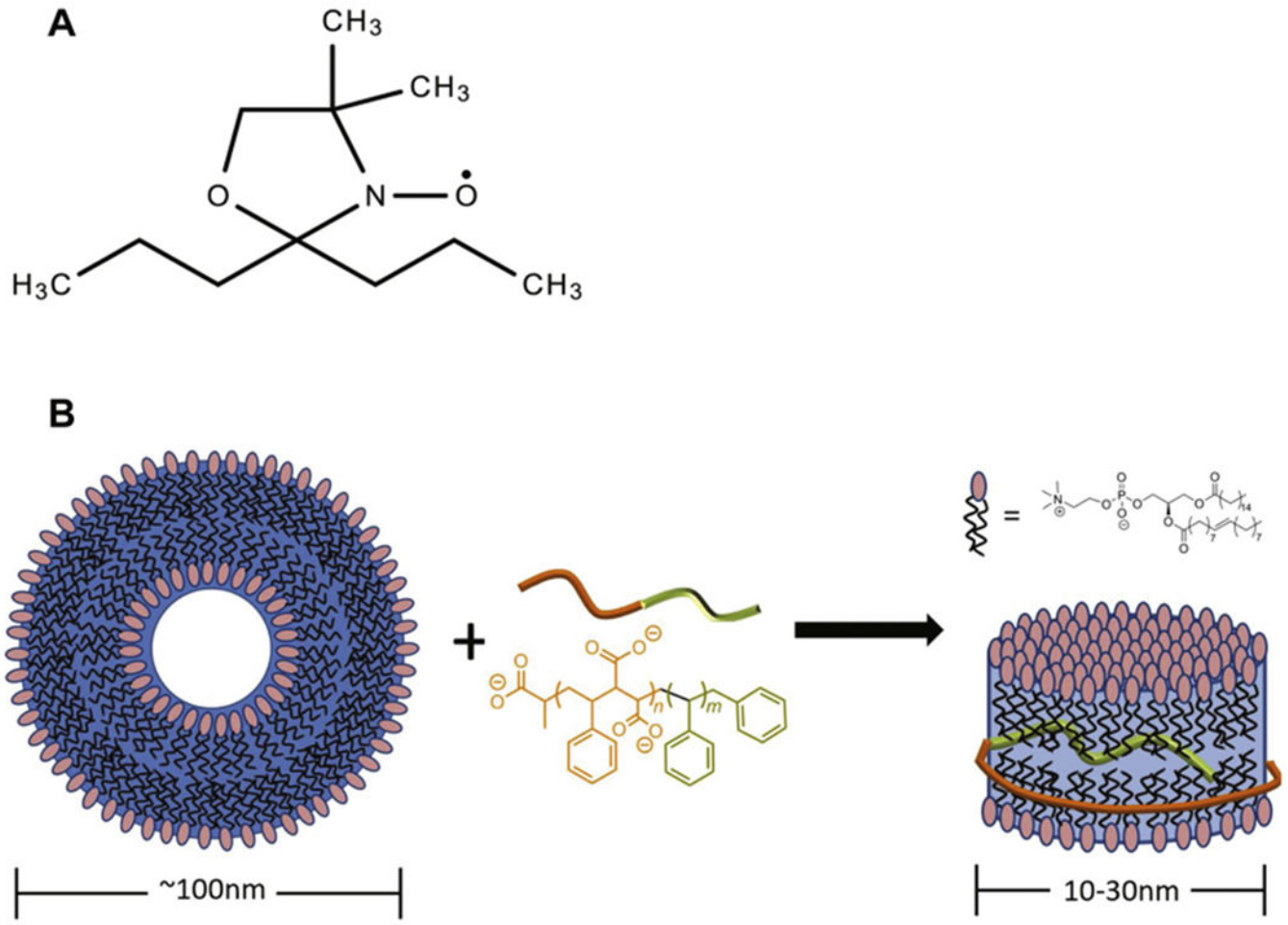

Fig. 1.

(A) Chemical structure of the DOXYL lipid spin label probe, (B) Cartoon representation of the addition of a SMA polymer to an intact vesicle and the structural implications of the addition to form the membrane RAFT SMALP.

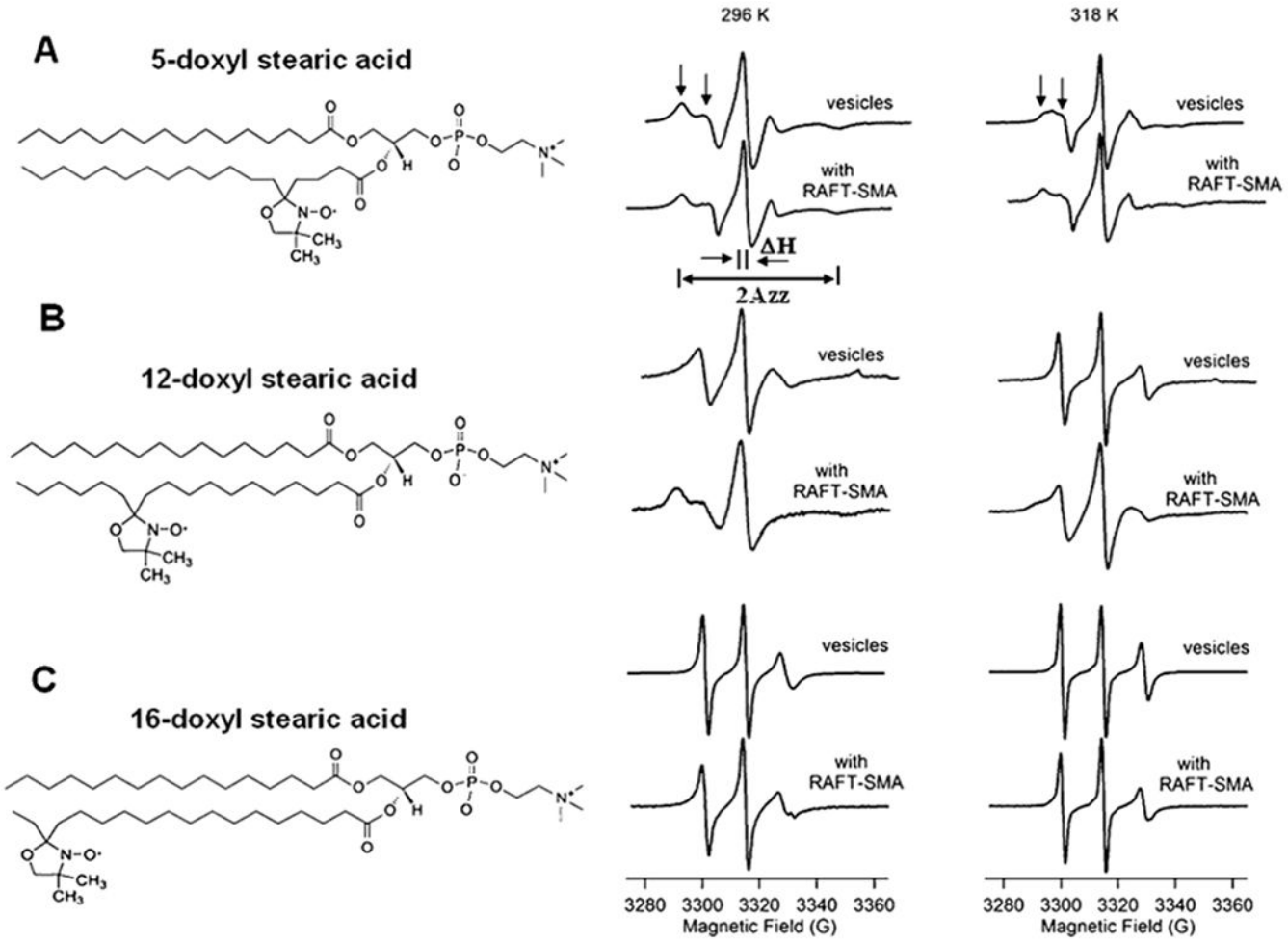

Fig. 2.

CW-EPR spectral data for each spin labelled carbon position: 5 (A), 12 (B), and 16 (C) DOXYL stearic acid at 296 K (23 °C) (middle panel) and 318 K (45 °C) (right panel). Left panel shows the cartoon representation of the spin labels attached to the 5^{th}, 12^{th}, and 16^{th} carbon of the acyl chain.

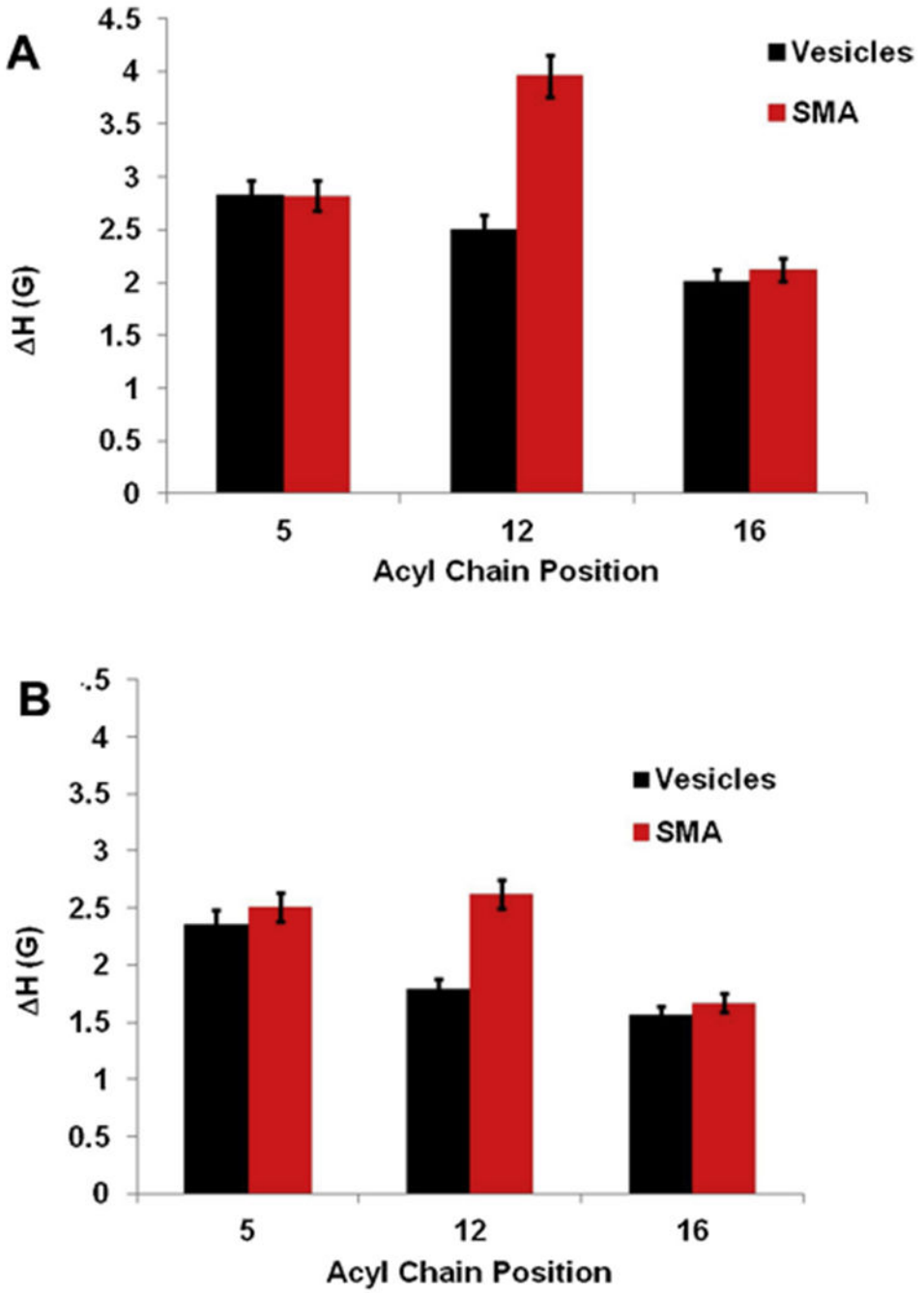

Fig. 3.

Central linewidth (ΔH) of EPR spectra as a function of spin labeled carbon position in vesicles and with the addition of SMA at temperatures Room Temperature (296 K) (23 °C) (A) 318K (45 °C) (B). The error bars represent uncertainties (standard deviation) arising from the triple batch of sample preparations and data analysis.

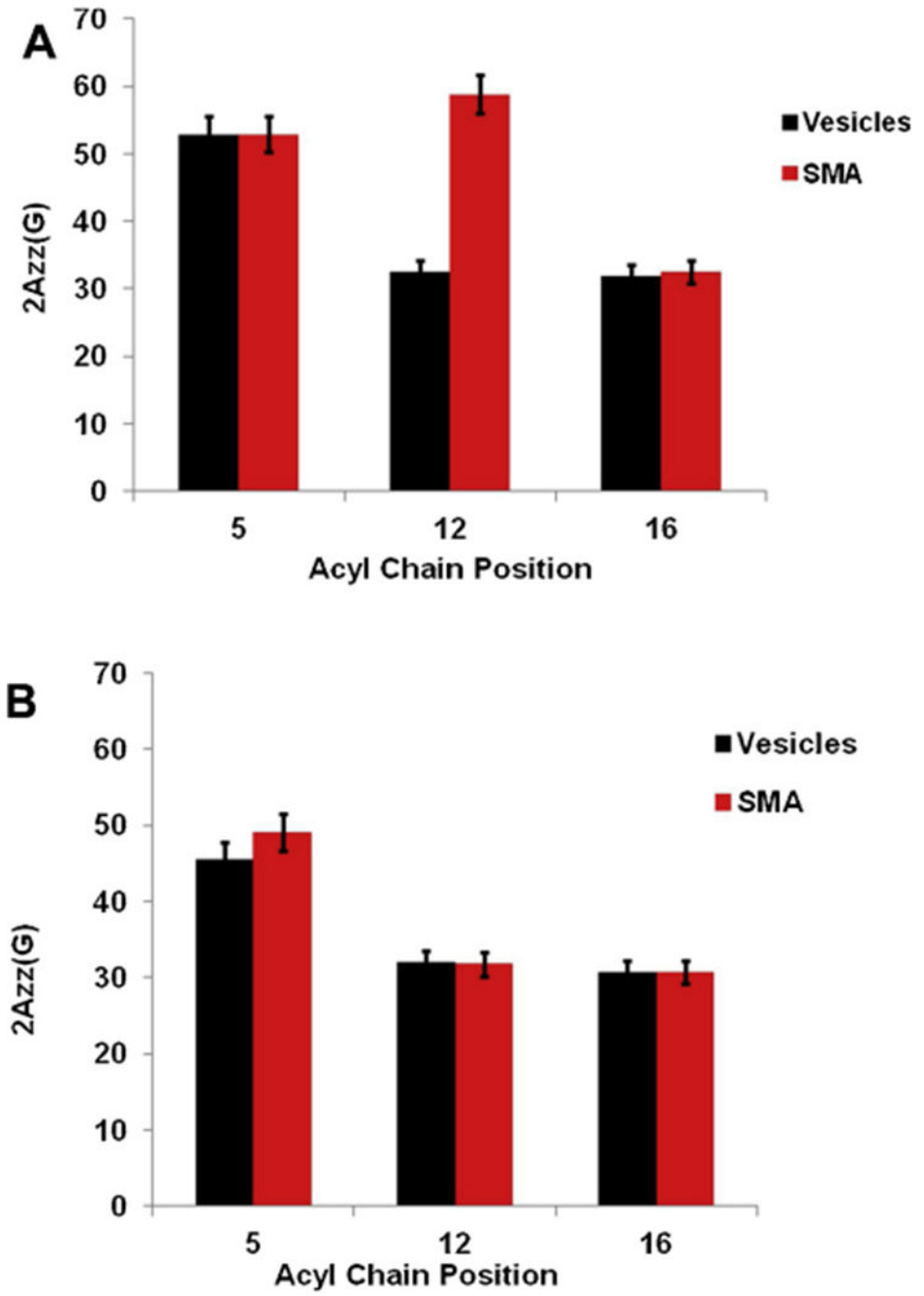

Fig. 4.

Spectral width ($2A_{zz}$) of EPR spectra as a function of spin labeled carbon position in vesicles and with the addition of SMA at temperatures 296 K (23 °C) (A) 318 K (45 °C) (B). The error bars represent uncertainties (standard deviation) arising from the triple batch of sample preparations and data analysis.

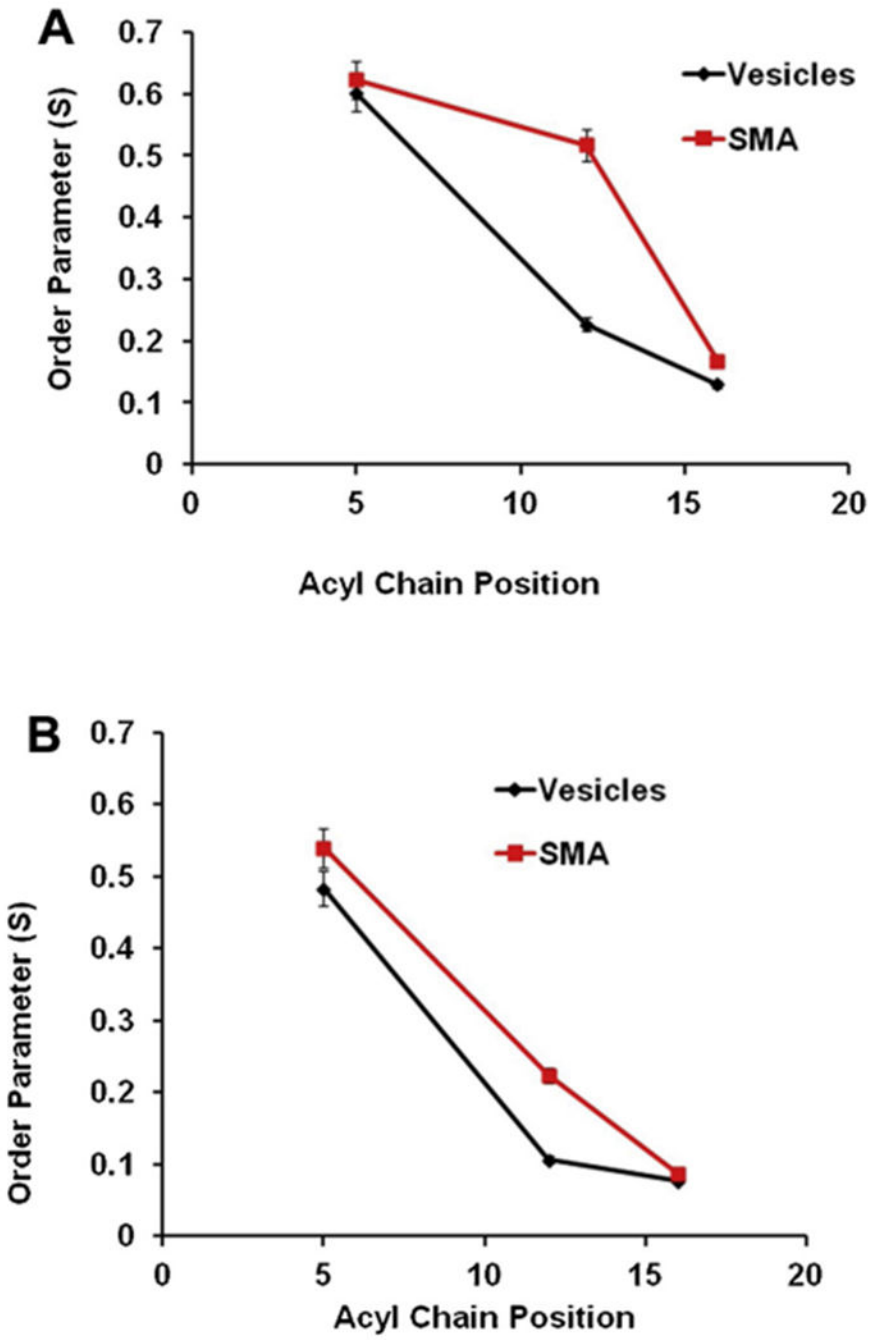

Fig. 5.

Order parameter (S) of EPR spectra as a function of spin labeled carbon position in vesicles and with the addition of SMA at temperatures 296 K (23 °C) (A) 318 K (45 °C) (B). The error bars represent uncertainties (standard deviation) arising from the triple batch of sample preparations and data analysis.

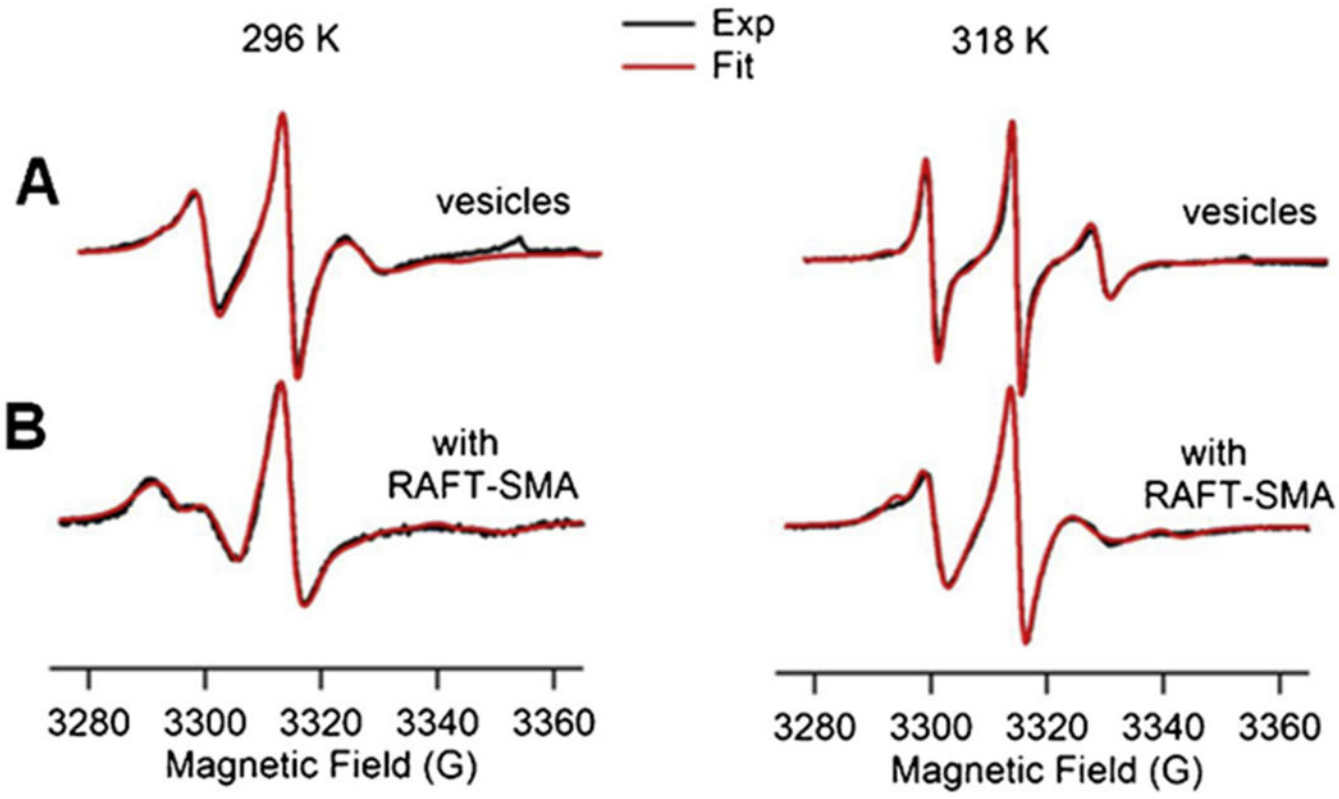

Fig. 6.

EPR spectral simulations for spin labeled acyl chain at carbon position 12 in vesicles (A) and with the addition of SMA (B) at temperatures 296 K (23 °C) (left panel) and 318 K (45 °C) (right panel).